ORIGINAL ARTICLE

U-turn time and velocity dependence on the wavelength of light: multicellular magnetotactic prokaryotes of different sizes behave differently

Marcos Venicio Gonçalves Sales[1] · Beatriz Silva Lima[1] · Daniel Acosta-Avalos[1]

Abstract

'*Candidatus* Magnetoglobus multicellularis' is a multicellular magnetotactic prokaryote found in the Araruama lagoon in Rio de Janeiro, Brazil. This microorganism shows a photokinesis that depends on the incident light wavelength, but that dependence can be canceled by the presence of radio-frequency (RF) electromagnetic fields. The present manuscript has as its aim to study the effect of light wavelength and RF fields on the U-turn time of '*Candidatus* Magnetoglobus multicellularis', a behavior more related to magnetotaxis. As the experiments were performed during the night, the microorganisms were greater in size than normal, indicating that they were in the process of division. Our results show that when normal in size, the microorganism's U-turn time is modified by the light wavelength (lower for blue light than for green and red light), but RF fields do not affect that U-turn time dependence on the light wavelength. For the microorganism in the process of division, we describe for the first time how the photokinesis and U-turn time dependence on the light wavelength disappear. It is proposed that methyl-accepting chemotaxis proteins are involved in that light wavelength dependence for the U-turn time, but still more studies are necessary to understand how RF fields cancel the photokinesis light wavelength dependence, but do not affect the dependence of the U-turn time.

Keywords Magnetotaxis · Multicellular magnetotactic prokaryote · Radical pair mechanism · U-turn · Monochromatic light · Photokinesis

Introduction

Magnetotaxis is the passive response to magnetic fields observed in a group of bacteria known as magnetotactic bacteria (MTB). Among the known MTB, there are a group of multicellular organisms known as Multicellular Magnetotactic Prokaryotes (MMP). There are two types: the spherical (sMMP) and the ellipsoidal (eMMP) (Abreu and Acosta-Avalos 2018). sMMP microorganisms are well studied and are found in almost all continents. '*Candidatus* Magnetoglobus multicellularis' (CMM) is a sMMP found in Rio de Janeiro, Brazil. It has a diameter of about 7 μm (between 5 μm and 9 μm) and is formed by an average number of 17 MTB, each one biomineralizing greigite magnetosomes arranged in linear chains (Abreu et al. 2007). The MTB composing the CMM are Gram-negative cells distributed in a spherical helix, being the helix axis the CMM motion axis (Keim et al. 2006). Phylogenetic analyses based on 16S rRNA genes sequences have shown that CMM is related to sulfate-reducing bacteria from the *Deltaproteobacteria* (Abreu et al. 2007). Transmission electron microscopy images show that the cells composing the CMM are arranged radially around an acellular internal compartment, found in the center of the organism, causing them to assume pyramidal shapes, with the CMM outer surface formed by the pyramid bases (Keim et al. 2006). The geometrical magnetic moment distribution around the CMM body produces a resultant magnetic moment directed in the helix axis (Acosta-Avalos et al. 2012). The CMM surface is covered by flagella which are helical tubes never as long as a helix turn (Silva et al. 2007). In Rio de Janeiro, Brazil, CMMs are South-seeking, meaning that they swim contrary to the magnetic field direction. The magnetotactic swimming trajectories of CMMs have been studied and characterized

✉ Daniel Acosta-Avalos
   dacosta@cbpf.br

1   Centro Brasileiro de Pesquisas Físicas, CBPF, Rua Xavier
    Sigaud 150, Urca, Rio de Janeiro, RJ 22290-180, Brazil

as cylindrical helixes (Keim et al. 2018), with the helix axis oriented to the magnetic field. The study of magnetotactic trajectories in MMPs has shown that magnetotaxis functions in a different way in CMMs when compared to uncultured MTB (De Melo et al. 2020) and that CMMs present photokinesis that is mediated by a radical-pair mechanism, a mechanism that is involved in light-dependent magnetoreception (De Melo and Acosta-Avalos 2017a).

It has been shown that CMMs are sensitive to low-intensity monochromatic light. Experiments were done measuring the mean velocity ΔS/Δt for monochromatic light (blue—469 nm, green—517 nm, and red—628 nm), and it was observed that there is an increase for the velocities under red light and a decrease in the velocities under green light when compared to the velocities under blue and white light (Azevedo et al. 2013). Changes in magnetic field and in the light intensity also change the relation among the velocities, meaning that the sensitivity to monochromatic light depends on the magnetic field value (Azevedo and Acosta-Avalos 2015). Azevedo et al. (2013) showed also that the U-turn time changes in the presence of monochromatic light, with the time lower for green light illumination than the time for the other monochromatic lights used. This dependence of the U-turn time on the wavelength of the illumination light has not been studied further. In the present manuscript, the axial velocity was measured in U-turn trajectories, assuming that sMMPs move in helical trajectories. U-turn times were measured under different monochromatic light conditions with the aim of confirming the results of Azevedo et al. (2013) about the U-turn time, and RF fields were applied simultaneously with the aim of investigating if radical-pair mechanisms influence the effect of monochromatic light on the U-turn in the same way it affects photokinesis (De Melo and Acosta-Avalos 2017a). Our aims were not completely fulfilled, because CMMs were in the division process and showed no photokinesis. This phenomenon is described for the first time.

Materials and methods

Microorganisms

Uncultured spherical multicellular magnetotactic prokaryotes were collected in Araruama lagoon (22°52′S, 42°20′W) located in Rio de Janeiro, Brazil. The sediments were collected and maintained in a glass aquarium in our lab in Rio de Janeiro city. Samples in the aquarium stayed alive by about 3 months, and it was necessary to collect a new sample after that time. The local geomagnetic parameters in Rio de Janeiro are: horizontal component = 18 µT, vertical component = − 15 µT, and total intensity = 23 µT.

To concentrate MMPs for the experiments, a sub-sample was transferred to a specially designed flask containing a lateral capillary aperture and a small magnet generating a magnetic field aligned to the capillary aperture (Lins et al. 2003). The studied MMPs were South-seeking and swam towards the capillary facing the North pole of a magnet. After 5 min, samples were collected with a micropipette.

U-turn recordings

The U-turn technique has been used to estimate the magnetic moment of magnetotactic microorganisms (Esquivel and Lins de Barros 1986). This trajectory is observed in the following situation: magnetotactic microorganisms are concentrated in the water drop border, for observation in an optical microscope, in the presence of a uniform magnetic field in the proper direction for a North- or South-seeking microorganism, when the magnetic field inverts its direction the magnetotactic microorganisms start to swim following the new direction, then a new magnetic inversion to the original direction makes the microorganism swim with a trajectory with a U form until the velocity became parallel to the new magnetic field direction (Fig. 1a). Theoretically, assuming that the only influences are the magnetic and hydrodynamic torques, in the Low Reynolds number regime, the total torque must be null and the following equation must be valid:

$$\text{mBsin}(\gamma) - 8\pi\eta R^3(d\gamma/dt) = 0, \qquad (1)$$

where mBsin(γ) is the magnetic torque and $- 8\pi\eta R^3(d\gamma/dt)$ is hydrodynamic torque or viscous drag torque. γ is the angle between the magnetic moment m and the magnetic field B, and it is assumed that the magnetic moment follows the trajectory direction, η is the water viscosity, and R is the microorganism radius. $8\pi\eta R^3$ is the viscous coefficient for a sphere and its expression is different for other body geometries. As Esquivel and Lins de Barros (1986) show, from the U-turn trajectory, two parameters can be used to estimate the magnetic moment of a MTB: the U-turn time τ and the U-turn radius. The U-turn radius is difficult to measure, because it is necessary that the MTB swims in the focal plane throughout the U-turn trajectory. The U-turn time is easier to measure from the trajectory and has been used in several studies to estimate the magnetic moment of MTBs (e.g., Perantoni et al. 2009; De Melo and Acosta-Avalos 2017b; Acosta-Avalos et al. 2019). From Eq. (1) it is possible to calculate the following expression for the U-turn time τ:

$$\tau = \left[8\pi\eta R^3/\text{mB}\right] \ln\left(2\text{mB}/kT\right), \qquad (2)$$

where kT is the thermal energy, k is the Boltzmann constant, and T is the absolute temperature.

Fig. 1 a Typical U-turn trajectory observed in a '*Candidatus* Mag-▶
netoglobus multicellularis' illuminated with blue light in Experiment
1. Axes are in pixels, because they are the crude data obtained from
ImageJ software. In the figure are indicated the beginning and the end
of the trajectory. The drop border is located to the left. **b** X coordinate
as a function of time. As it can be seen, the curve is composed by two
straight lines with inclination of different sign. **c** Derivative of X in **b**
with respect to time as a function of time. It is observed a transition
between the positive and negative inclinations. The U-turn time τ is
the time interval between both inclinations. In the figure, letter b indi-
cates the begin and letter e indicates the end of the interval of time. In
this case, τ = 0.45 s


The U-turn trajectories were recorded to calculate the
U-turn time τ. On the stage of an inverted microscope
(Nikon Eclipse TS100) were set a pair of coils connected
to a DC power supply and fixed to a glass microscope slide
where the collected drop with MMPs was placed. The lens
used had a magnification of 20× and numerical aperture
of 0.55 allowing the measurement of the MMP radius *R*.
The magnetic field generated by the coils was 0.2 mT and
0.3 mT. An electric circuit for changing the voltage polarity
(reversal of current) was connected between the power sup-
ply and coils, leading to the inversion of the magnetic field
direction when the button was turned to on or off. After two
magnetic field inversions, the MMP perform a U-turn move-
ment (Fig. 1a). To calculate τ, the following procedure was
performed: U-turn trajectories were recorded, with a rate
of 82 fps, in the inverted microscope with a digital camera
(Lumera Infinity 1). The coordinates of the U-turn trajecto-
ries were obtained using the software *ImageJ* (NIH—USA).
The coordinates were in pixel units and the conversion to μm
was done using a calibration ruler, which consists in a 1 mm
line divided in 100 parts. In the experimental set-up, the
external magnetic field is applied in the x direction, meaning
that the x coordinate of the U-turn in Fig. 1, as a function of
time, must be composed of two straight lines with different
slopes (Fig. 1b). The U-turn time τ must be the time neces-
sary for the change of slope and can be calculated through
the derivative *dx/dt* (Fig. 1c).

The axial velocity was measured analyzing the move-
ment before the magnetic field inversion associated with
the U-turn, assuming that the MTB trajectory is similar to a
cylindrical helix. In this case, if the helix axis is aligned to
the magnetic field direction, then the coordinates must have
the following parametrization:

$$x'(t) = x_0 + V_{ax} \cdot t \tag{3a}$$

$$y'(t) = y_0 + r \cdot \cos\left(2\pi f t + \phi_0\right), \tag{3b}$$

where x_0 and y_0 are initial values for the coordinates, V_{ax} is
the axial velocity, r is helix radius, f is the helix frequency,
and ϕ_0 is the phase constant. However, the trajectory is
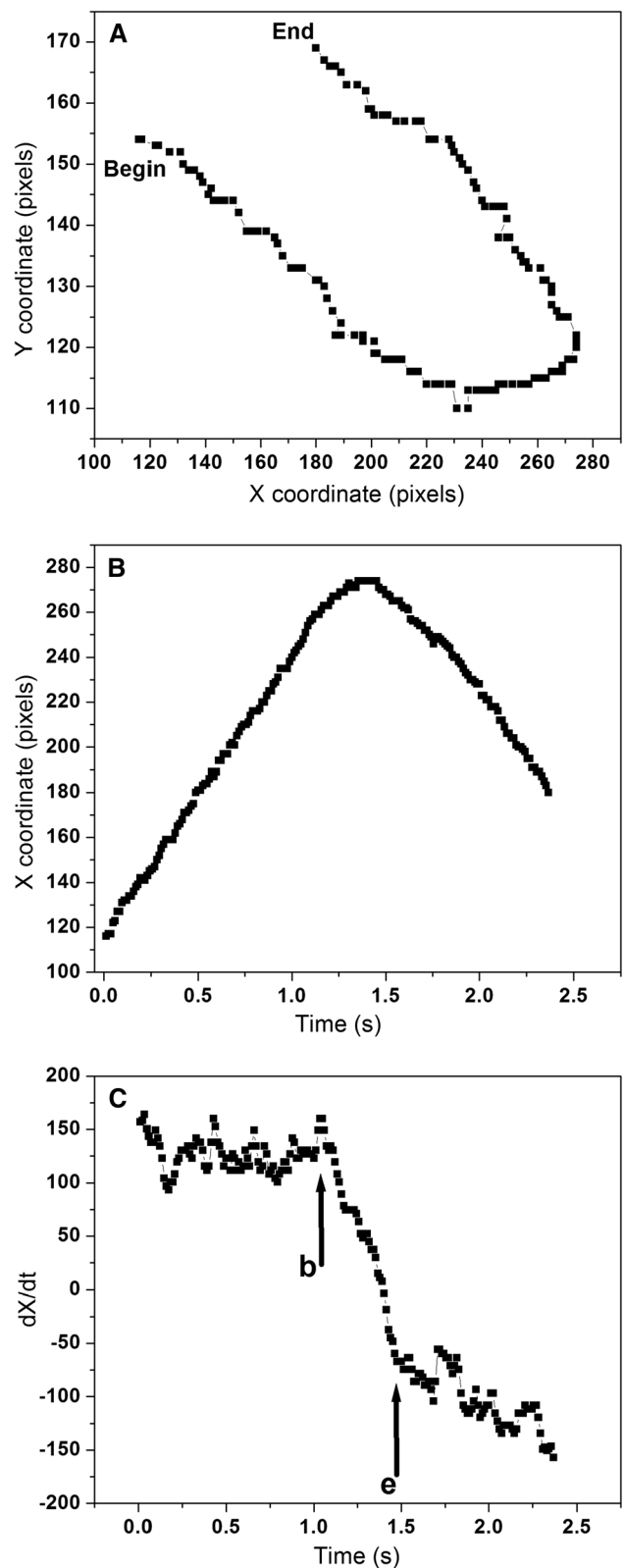
not fully parallel to the magnetic field direction because
of thermal perturbations that disorient the bacterial swim-
ming (Kalmijn 1981). If the trajectory is tilted relative to the

magnetic field by an angle θ, the coordinates must have the following expressions:

$$x(t) = x' \cos\theta + y' \sin\theta = r\sin\theta \cos\left(2\pi ft + \phi_0\right) + V_{ax} \cdot t \cdot \cos\theta \tag{4a}$$

$$y(t) = -x' \sin\theta + y' \cos\theta = r\cos\theta \cos\left(2\pi ft + \phi_0\right) - V_{ax} \cdot t \cdot \sin\theta. \tag{4b}$$

The observed coordinates x and y as a function of time must be oscillating functions with linear tendencies. If θ is near to 0°, then $x(t)$ must be similar to a straight line and $y(t)$ must be an oscillating function with an inclination. The inclinations of x and y correspond to $V_x = V_{ax} \cdot \cos\theta$ and $V_y = V_{ax} \cdot \sin\theta$, respectively, and $V_{ax} = (V_x^2 + V_y^2)^{1/2}$. The inclination for each coordinate is calculated through a linear fit as a function of time for the curve before the magnetic field inversion. In general, it is not easy to calculate r and f, because the coordinate $y(t)$ has a complex oscillating behavior, similar to the sum of two oscillating functions with two frequencies and radiuses. Even with that complex oscillating behavior in $y(t)$, the axial velocity can be calculated from the time derivatives, as shown in Eqs. 4a and 4b.

Experiments with monochromatic light

Three different experiments were done on different dates, and they will be identified as Experiment 1 (Exp1) done at October 2017, Experiment 2 (Exp2) done at August 2018, and Experiment 3 (Exp3) done at October 2018. For each set of experiments, new CMMs were collected at Araruama Lagoon. All the experiments were performed during the night beginning at about 17:00 h. These experiments were conducted in a dark room with the illumination in the microscope being done by a monochromatic LED lamp (blue: 469 nm, green: 517 nm, and red: 628 nm) (Fig. 2) positioned in the same place of the tungsten microscope lamp as has been done by De Melo and Acosta-Avalos (2017a). The power of each monochromatic light was maintained in 120 µW at the glass slide and measured using a power meter (Newport Optical Power Meter Model 1916-C). The tungsten lamp light was used as a control. Experiments 1 and 2 were performed with a frame rate of 82 fps and magnetic field of 0.2 mT, while Experiment 3 was performed with a frame rate of 54 fps and magnetic field of 0.3 mT, because on that day, the CMMs behaved differently from the other two experiments. De Melo and Acosta-Avalos (2017a) showed that monochromatic light's effect on photokinesis can be canceled by radio-frequency electromagnetic fields. In the present work, radio-frequency was also applied to observe its effect on the U-turn time. The frequency was calculated using the expression for the Zeeman resonance frequency:
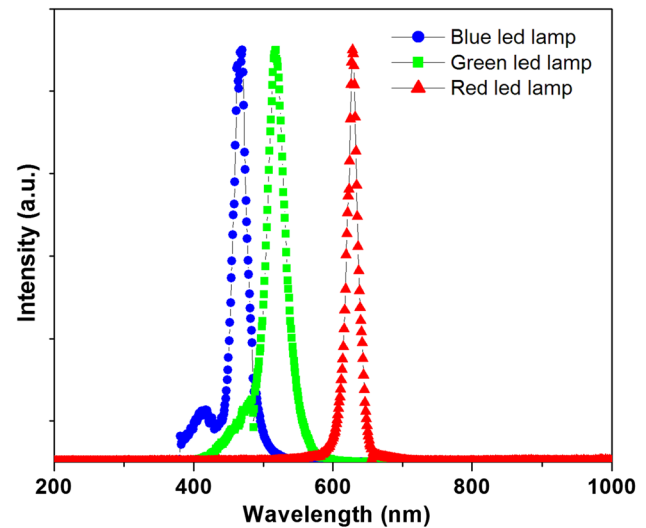

Fig. 2 Spectral emission of the monochromatic LED lamps used in the experiment: blue lamp: maximum = 469 nm, FWHM = 22 nm; green lamp: maximum = 517 nm, FHWM = 28 nm; red lamp: maximum = 628 nm, FWHM = 16 nm. All spectra are normalized to their respective maximums

$$f_{RF} = \left(28.025 \text{ MHz} \times \text{mT}^{-1}\right) \times B_0, \tag{5}$$

where B_0 is the magnetic field applied by the pair of coils. For Experiments 1 and 2, the RF field has frequency of 5.6 MHz and for Experiment 3 a frequency of 8.4 MHz. The procedure to generate the RF electromagnetic field is the same described by De Melo and Acosta-Avalos (2017a).

In all the experiments, the microorganism size R, the axial velocity V_{ax}, the U-turn time τ as a function of the light wavelength illumination condition, and with or without the presence of RF fields were calculated.

All graphics and analysis were done using the software *Microcal Origin* and the statistics with the software *GraphPad InStat* and *Oriana* for circular statistics.

Results and discussion

CMM size

Table 1 shows the statistics of the diameters measured in the CMMs observed in each experiment. The values correspond with the experiments done in the presence of a 0.2 mT magnetic field. Figure 3 shows that the distributions are Normal. The values observed for diameters are in agreement with the size observed previously in CMMs from Araruama Lagoon (Abreu et al. 2007; De Melo and Acosta-Avalos 2017b). It is observed that Exp1 diameters are lower than diameters for Exp2 and Exp3 (Fig. 4). CMM has a life cycle characterized by initially doubling its volume before starting a splitting

Table 1 Statistics for '*Candidatus* Magnetoglobus multicellularis' size in Experiment 1 (Exp1), Experiment 2 (Exp2), and Experiment 3 (Exp3)

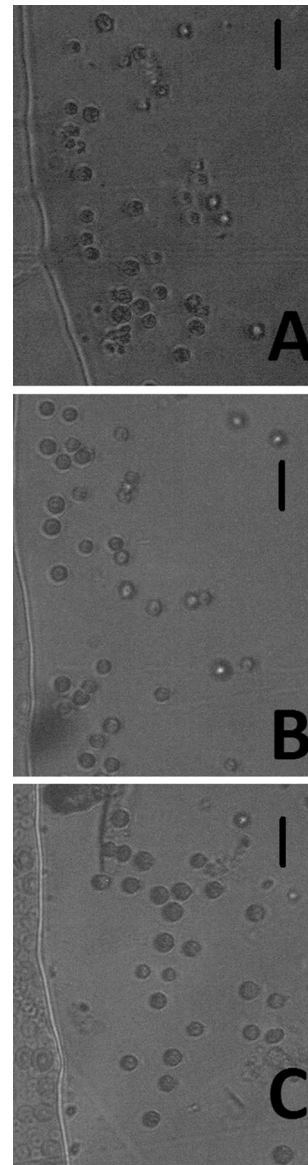|	D (μm)	SE	Range	N
Exp1	5.85[a]	0.67	4.23–7.82	340
Exp2	6.77[b]	0.72	4.61–8.68	243
Exp3	7.77[c]	0.99	5.61–10.58	247

D is the diameter, SE is the standard error, Range is the minimum and maximum values in the group, and N is the number of microorganisms measured. Different letters in column D represent the statistic difference (ANOVA test, $p < 0.05$)
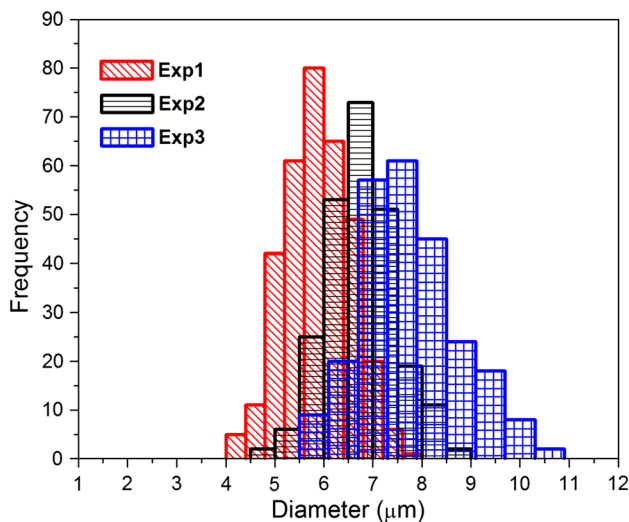
Fig. 3 Histogram for the diameters of '*Candidatus* Magnetoglobus multicellularis' for the three experiments done in the present manuscript. Exp1 = Experiment 1. Exp2 = Experiment 2. Exp3 = Experiment 3. The statistics for the diameters are in Table 1

Fig. 4 '*Candidatus* Magnetoglobus multicellularis' observed by optical microscopy in the border of the water drop. **a** Microorganisms observed in Experiment 1. **b** Microorganisms observed in Experiment 2. **c** Microorganisms observed in Experiment 3. The scale bar in all images represents 20 μm

process by enlarging its body and twisting at its middle to produce two equal daughters (Keim et al. 2006). Doubling the volume means that the relation among the initial microorganism diameter d_I and the pre-splitting microorganism diameter d_P must be (Perantoni et al. 2009):

$$\left(d_P/d_I\right) = (2)^{1/3} \approx 1.26. \qquad (6)$$

Observing the average values in Table 1, we get the values $(d_{E2}/d_{E1}) = 1.16$ and $(d_{E3}/d_{E1}) = 1.33$. From those values, it can be considered that the microorganisms in Experiments 2 and 3 are microorganisms that already doubled their volume to start the division process. It has been shown that in environmental samples containing CMMs, collected during the day (13:00 h) and night (21:00 h), the microorganisms move downward at night and the number of CMMs in the process of division during the night was higher, suggesting that the CMM life cycle might be under control of a circadian rhythm (Abreu et al. 2014). Following findings described in the paper of Abreu et al. (2014), the fact that our experiments were performed during the night, and the size relations among Exp1 CMMs and Exp2—Exp3 CMMs show that the majority of the CMMs studied in the present manuscript were in the process of division.

Light-dependent photokinesis

Table 2 shows the values of V_{ax} for the three experiments in the different illumination conditions. As can be seen, a light-dependent photokinesis is only observed in Exp1 where CMMs are at their normal size. The velocity under red light continues to be bigger than that under green light, but the relation between velocities under white and blue light is different than has been observed at 0.4 mT by De Melo and Acosta-Avalos (2017a) or 0.14 mT by Azevedo et al. (2013), where white and blue give rise to the same translation velocity value. Azevedo and Acosta-Avalos (2015) showed that there is a complex relation among the translation velocity, the magnetic field intensity and the monochromatic light power, and in some conditions, blue and red light can give rise to similar velocity values, but green is always lower. That is observed also in Table 2 for Experiment 1. The RF field affected the velocity of CMMs under white, green, and red illumination but not under blue illumination, as De Melo and Acosta-Avalos (2017a) also showed. As Experiment 1 also was performed during the night, it is interesting to observe the results obtained with an experiment done during the day (morning at about 10:00 h) with CMMs from the same sample. The velocity was measured using the same procedure as described above, in the presence of a magnetic field of 0.5 mT, and the result was: for blue light $V_{ax} = 122.7 \pm 22.2$ µm/s ($N = 55$), for green light $V_{ax} = 99.2 \pm 23.8$ µm/s ($N = 30$), and for red light $V_{ax} = 152.1 \pm 32.3$ µm/s ($N = 55$) ($V_{ax} = $ mean $\pm$ standard deviation; all values are statistically different: ANOVA test $p < 0.05$). Those results are in accord with the light wavelength-dependent photokinesis reported by Azevedo et al. (2013), Azevedo and Acosta-Avalos (2015) and De Melo and Acosta-Avalos (2017a). The results in Experiment 1 concerning the RF effect on the photokinesis are not comparable with the results showed by De Melo and Acosta-Avalos (2017a), because the CMMs in the Experiment 1 are physiologically different, since they are preparing for the division process. In Experiment 2, the photokinesis changes. In this case, red light maintains lower velocities than blue and green light, and the RF field only acts over green light illumination. When the size increases more, as in Experiment 3, the photokinesis disappears and the RF field no longer affects the velocity of the microorganisms. The results of Exp2 in Table 2 shows that in certain size conditions, before the beginning of the division process, light still affects the velocity but not through a radical-pair mechanism, and when the size is more than the expected doubling of normal size, the radical-pair mechanism associated with photokinesis disappears. Table 2 also shows that there is an increase in the velocity from Exp2 to Exp3, indicating some sort of relation among the microorganism velocity and volume (Fig. 5). It is interesting that for each experiment, there is no significant correlation between diameter and velocity (Pearson correlation test: $p > 0.05$ in all cases). Figure 3 shows that the increase in diameter determines an increase in velocity, perhaps because in this case, greater CMMs in Experiments 2 and 3 have more cells and more flagella than CMMs in Experiment 1, as expected for CMMs in the division process, increasing their propulsion power.

U-turn time

Table 3 shows the U-turn time τ measured in all the illumination conditions in the three experiments. As can be observed, in Experiment 1, there is a dependence of τ on the wavelength, as was reported by Azevedo et al. (2013). The difference observed between that study and the present report is that Azevedo et al. (2013) used a different methodology to estimate the U-turn time and monochromatic

Table 2 Statistics for axial velocities V_{ax} in Experiment 1 (Exp1), Experiment 2 (Exp2), and Experiment 3 (Exp3), as a function of the light wavelength and the presence of RF fields

Light illumination	V_{ax} (µm/s)		
	Exp1	Exp2	Exp3
White	47.3 ± 1.8^A (41)[S]		
White + RF	68.7 ± 2.3^a (40)		
Blue (469 nm)	73.5 ± 3.4^B (46)[NS]	95.3 ± 2.4^A (36)[NS]	109.5 ± 3.2^A (41)[NS]
Blue + RF	69.5 ± 2.6^a (40)	101.2 ± 2.8^a (40)	113.1 ± 3.8^a (39)
Green (517 nm)	52.1 ± 2.9^A (41)[S]	88.4 ± 2.4^A (41)[S]	99.6 ± 3.3^A (41)[NS]
Green + RF	82.4 ± 2.6^b (46)	95.6 ± 2^a (40)	105.1 ± 4.3^a (41)
Red (628 nm)	64.6 ± 2.2^B (45)[S]	72.5 ± 2.8^B (40)[NS]	103.8 ± 3.2^A (40)[NS]
Red + RF	73.9 ± 2^{ab} (42)	79 ± 3.2^b (41)	102.1 ± 2.5^a (42)

In each column is represented the average value and its standard error, and between parentheses the number of microorganisms measured. Different letters over the standard error value represent the statistical difference (ANOVA test, $p < 0.05$): uppercase letters stand for experiments without RF field and lowercase letters stand for experiments with RF fields. Letters over the parentheses are to show the statistical difference between experiments with fixed light wavelength with and without RF fields (t-Student test, $p < 0.05$): S = statistical significant difference and NS = No statistical difference
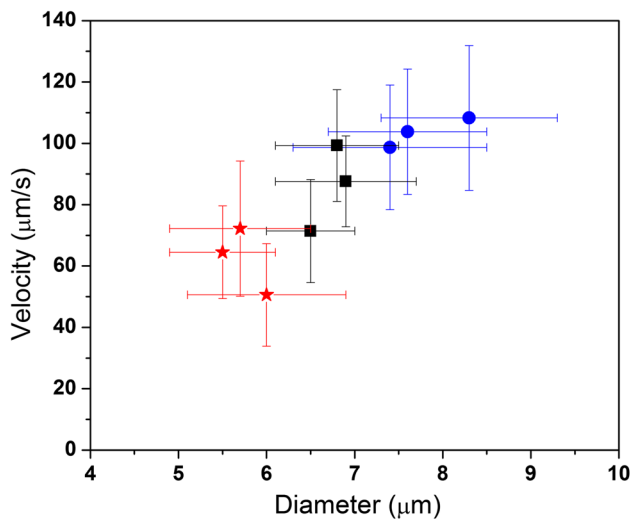
Fig. 5 Velocity as a function of the diameter for blue, green, and red illuminations in Experiments 1, 2, and 3. Symbols are related to the Experiment: stars for Exp1, squares for Exp2, and dots for Exp3. The coordinates in each symbol are the average values for velocity and diameter for each experiment, and bars indicate the corresponding standard deviation

light with different power, producing as a result a U-turn time for green light lower than that for blue, yellow, and red light illumination, which were statistically similar. In Table 3, it is observed that with red light the value of τ is lower than that for blue and green light, which are statistically similar, and also it is observed that the RF field does not affect the U-turn time for any monochromatic light, different than was observed with the velocity. When the size increases in Experiments 2 and 3, the U-turn time does not change with the monochromatic light and with the RF field.

Discussion

The present manuscript shows that under normal size conditions, before the beginning of the division process, CMM presents a photokinesis that is canceled by RF fields whose frequency is calculated through the Zeeman resonance formula, indicating the involvement of a radical-pair mechanism. Experiments done during the day in the present manuscript showed the usual light wavelength-dependent photokinesis in CMMs (Azevedo et al. 2013; Azevedo and Acosta-Avalos 2015; De Melo and Acosta-Avalos 2017a). During the performance of the present experiments, we were not aware of the comment of Abreu et al (2014) about the prevalence of CMMs in the division process in samples collected during the night, and for us, it was a surprise to correlate the disappear of light wavelength-dependent photokinesis with the increase of the CMM size. When the microorganism size increases, both photokinesis and the RF field influence disappear and an increase in translation velocity is observed (Fig. 3). The fact that the division process produces the disappearance of photokinesis must be associated with a higher production of proteins needed for cell division that block the action of chromophores involved in CMM photokinesis. Up to now, it is not known what chromophores are responsible for the observed photokinesis in CMM. Its cryptochrome is discounted, because it absorbs blue light and is sensitive to RF fields in that wavelength, but our results show that, in CMM, the chromophore involved is not sensitive to blue light. In some way, during the division process, the photokinesis chromophore of CMM is involved in another function or is not produced.

Our results also show that the U-turn time is affected by the light wavelength, but it is insensitive to RF fields in the Zeeman resonance frequency. When the size increases, the

Table 3 Statistics for the U-turn time τ in Experiment 1 (Exp1), Experiment 2 (Exp2), and Experiment 3 (Exp3), as a function of the light wavelength and the presence of RF fields

Light illumination	τ (s)		
	Exp1	Exp2	Exp3
White	0.34 ± 0.02^A (41)[NS]		
White + RF	0.37 ± 0.2^a (40)		
Blue (469 nm)	0.57 ± 0.03^B (46)[NS]	0.37 ± 0.01^A (40)[NS]	0.43 ± 0.03^A (41)[NS]
Blue + RF	0.63 ± 0.06^b (40)	0.35 ± 0.02^a (40)	0.45 ± 0.02^a (40)
Green (517 nm)	0.52 ± 0.04^B (41)[NS]	0.35 ± 0.02^A (41)[NS]	0.45 ± 0.03^A (41)[NS]
Green + RF	0.47 ± 0.03^a (46)	0.36 ± 0.02^a (40)	0.44 ± 0.03^a (41)
Red (628 nm)	0.40 ± 0.02^A (45)[NS]	0.35 ± 0.02^A (42)[NS]	0.51 ± 0.03^A (40)[NS]
Red + RF	0.38 ± 0.02^a (42)	0.36 ± 0.02^a (43)	0.49 ± 0.03^a (42)

In each column is represented the average value and its standard error, and between parentheses the number of microorganisms measured. Different letters over the standard error value represent the statistical difference (ANOVA test, $p < 0.05$): uppercase letters stand for experiments without RF field and lowercase letters stand for experiments with RF fields. Letters over the parentheses are to show the statistical difference between experiments with fixed light wavelength with and without RF fields (t-Student test, $p < 0.05$): S = statistical significant difference and NS = No statistical difference

dependence on the light wavelength disappears and a unique behavior is observed. We deduce that the mechanisms related to the light wavelength-dependent photokinesis and U-turn in CMM are different. The U-turn is considered to be mediated only by the magnetic torque among the resultant magnetic moment and the external magnetic field (Esquivel and Lins de Barros 1986). Some studies have considered that traditional U-turn analysis lacks a necessary flagellar contribution that could be added to the differential equation describing it (Pichel et al. 2018) or that a correction in the hydrodynamic torque coefficient may be required (Chen et al. 2018). The magnetic moment calculated through Eq. (2) for the U-turn time τ is shown in Table 4 for Experiment 1. It is observed that the average magnetic moment has a dependence on the light wavelength, but the magnetic moment is a material property that never has been observed to change with irradiation of low power light. An interpretation of the variations in τ observed in Table 3 is that the monochromatic light is affecting the flagellar function, and introducing perturbations that affect the U-turn dynamics. As the microorganism movement is controlled by the flagella, then the light irradiation might only increase the flagellar perturbation and not cancel it, producing an increase in the effective temperature T_{Eff} and a decrease in the rate $mB/k_B T_{Eff}$ observed in Eq. (2). That effect must produce as a result wrong estimates of the magnetic moment lower than its real value. That was observed by Rosenblatt et al. (1982) when designed a birefringence technique to study the magnetic moment of *Aquaspirillum magnetotacticum*. They observed that the estimated magnetic moment of live cells is always lower than that of dead cells, and proposed that a hydrodynamic effect can be the source of the effect: the swimming of the bacteria can affect the orientations of nearby bacteria in some way and have the effect of increasing the effective temperature, producing a non-thermal perturbation as estimated through $k_B T_{Eff}$. In Table 4, it is observed that for green and red light, the magnetic moment values are greater than for blue light. The magnetic moment histogram for each distribution in Table 3 shows a non-Gaussian distribution with two maxima in each case: 15×10^{-15} Am^2 and 27×10^{-1} Am^2

for blue light; 24×10^{-15} Am^2 and 44×10^{-15} Am^2 for green light; 24×10^{-15} Am^2 and 46×10^{-15} Am^2 for red light and 34×10^{-15} Am^2 and 55×10^{-15} Am^2 for white light. Previous studies have shown that the CMM magnetic moment estimated through the U-turn technique, and using white light, is distributed in a curve with two maxima at about 10×10^{-15} Am^2 and 20×10^{-15} Am^2 (Perantoni et al. 2009). However, a mathematical model for the magnetic moment distribution in CMM calculates a magnetic moment of 23×10^{-15} Am^2 for a microorganism with 15 cells and assuming that each cell has a magnetic moment of 1.8×10^{-15} Am^2 (Acosta-Avalos et al. 2012). It is interesting to observe that that theoretical magnetic moment value must be lower than the real one, because the observed average value of the cells in CMM is 17 but for CMM organisms composed of up to 30 MTB (Keim et al. 2006). The results in Table 4 can be interpreted as for green and red light the non-thermal perturbation decreases in comparison to the blue light perturbation. It is known that magnetotactic bacteria from the genus *Magnetospirillum* possess diversified photoreceptor genes that may be responsible for phototaxis, including genes that encode phytochrome-domain photoreceptors that induce red/far-red light phototaxis (Wang et al. 2019). Perhaps, phytochrome photoreceptors are involved in the observed CMM red light photokinesis (Azevedo et al. 2013). An interesting result was reported by Chen et al. (2018). They studied the participation of the methyl-accepting chemotaxis protein *amb0994* in the magnetotaxis of *Magnetospirillum magneticum* AMB-1, comparing the behavior of wild-type bacteria and mutants with suppressed *amb0994*. Zhu et al. (2014) showed that *amb0994* is used by AMB-1 bacteria to sense the torque and actively regulate the flagellar rotation bias to align its orientation with the magnetic field. Chen et al. (2018) showed that after a magnetic field inversion of direction, the U-turn parameters are not equal between both AMB-1 wild type and mutants: mutants present higher velocities than wild type and mutants present lower U-turn times than wild type. These differences are interpreted through the interference of *amb0994* in the flagellar function, interference that is not observed in the mutant. In other words, the results of Chen et al. (2018) show that the non-thermal perturbation is generated by the flagellar action of the *amb0994* protein activated by the magnetic torque. MMPs are composed by magnetotactic bacteria, and perhaps something similar can be happening here: illumination with green and red light should interfere in the function of a similar protein of the methyl-accepting chemotaxis protein group, decreasing or blocking the effect of that protein on the flagellar function, increasing or decreasing the velocity and increasing the estimated magnetic moment through the elimination of the non-thermal perturbation. The suppression of that effect when CMMs are starting their division process could be related to a non-production of those proteins, because they need to produce more proteins related to the division process. However, it is not clear how the same

Table 4 Mean values of 'Candidatus Magnetoglobus multicellularis' magnetic moments as a function of the light wavelength

Light illumination	Magnetic moment ($\times 10^{-15}$ Am^2)	SE	N
White	48.7[a]	2.9	39
Blue (469 nm)	23.7[b]	1.5	41
Green (517 nm)	34.8[c]	2.5	40
Red (628 nm)	35[c]	2.1	45

Magnetic moments were estimated using Eq. (2). Data are related to the Experiment 1 and without RF field application. SE = standard error. N = sample size. Different letters in column D represent the statistic difference (ANOVA test, $p < 0.05$)

protein can be affected by RF electromagnetic fields during photokinesis and is not during the U-turn. This hypothesis must be explored in future studies on CMM behavior.

Conclusion

The present manuscript described for the first time the unexpected result of the absence of light wavelength-dependent photokinesis in experiments performed during the night in CMMs when the microorganisms are involved in the division process. Our results confirmed the effect of RF electromagnetic fields on photokinesis induced by green and red light, and show that the U-turn time is affected by the wavelength of the light irradiation, but is not affected by RF fields. However, the last results must be performed again in experiments done during the day. We hypothesize that methyl-accepting chemotaxis proteins are involved in the light effect on the U-turn and perhaps on photokinesis but more studies are necessary to understand how RF fields affect only photokinesis and not the U-turn time in Experiment 1. As the greater CMM sizes observed in Experiments 2 and 3 are related to the beginning of the CMM division process, it is possible that the observed insensitivity to the light wavelength is related to the non-production of proteins related to the light wavelength sensitivity, because they need to produce more proteins related to the division process.

Data availability Under request, the authors can send the videos and data that support our research.

Compliance with ethical standards

Conflict of interest Authors declare no conflicts of interest.

References

Abreu F, Acosta-Avalos D (2018) Biology and Physics of magnetotactic bactéria. In: Blumenberg M, Shaaban M, Elgaml A (Eds.) Microorganisms. IntechOpen. https://doi.org/10.5772/intechopen.79965

Abreu F, Martins JL, Silveira TS, Keim CN, Lins de Barros HGP, Gueiras-Filho F, Lins U (2007) 'Candidatus Magnetoglobus multicellularis', a multicellular magnetotactic prokaryote from a hypersaline environment. Int J Syst Evol Microbiol 57:1318–1322

Abreu F, Morillo V, Nascimento FF, Werneck C, Cantão ME, Ciapina LP, Almeida LGP, Lefevre CT, Bazylinski DA, Vasconcelos ATR, Lins U (2014) Deciphering unusual uncultured magnetotactic multicellular prokaryotes through genomics. ISME J 8:1055–1068

Acosta-Avalos D, Azevedo LMS, Andrade TS, Lins de Barros H (2012) Magnetic configuration model for the multicellular magnetotactic prokaryote Candidatus Magnetoglobus multicellularis. Eur Biophys J 41:405–413

Acosta-Avalos D, Figueiredo AC, Conceição CP, da Silva JJP, Aguiar KJMSP, Medeiros ML, Nascimento M, De Melo RD, Sousa SMM, Lins de Barros H, Alves OC, Abreu F (2019) U-turn trajectories of magnetotactic cocci allow the study of the correlation between their magnetic moment, volume and velocity. Eur Biophys J 48:513–521

Azevedo LV, Acosta-Avalos D (2015) Photokinesis is magnetic field dependent in the multicellular magnetotactic prokaryote Candidatus Magnetoglobus multicellularis. Antonie Van Leeuwenhoek 108:579–585

Azevedo LV, Lins de Barros H, Keim CN, Acosta-Avalos D (2013) Effect of light wavelength on motility and magnetic sensibility of the magnetotactic multicellular prokaryote 'Candidatus Magnetoglobus multicellularis'. Antonie van Leewenhoek 104:405–412

Chen H, Zhang SD, Chen L, Cai Y, Zhang WJ, Song T, Wu LF (2018) Efficient genome editing of Magnetospirillum magneticum AMB-1 by CRISPR-Cas9 system for analyzing magnetotactic behavior. Front Microbiol 9:1569

De Melo RD, Acosta-Avalos D (2017a) Light effects on the multicellular magnetotactic prokaryote 'Candidatus Magnetoglobus multicellularis' are cancelled by radiofrequency fields: the involvements of radical pairs mechanisms. Antonie Van Leeuwenhoek 110:177–186

De Melo RD, Acosta-Avalos D (2017b) The swimming polarity of multicellular magnetotactic prokaryotes can change during an isolation process employing magnets: evidence of a relation between swimming polarity and magnetic moment intensity. Eur Biophys J 46:533–539

De Melo RD, Leão P, Abreu F, Acosta-Avalos D (2020) The swimming orientation of multicellular magnetotactic prokaryotes and uncultured magnetotactic cocci in magnetic fields similar to the geomagnetic field reveals differences in magnetotaxis between them. Antonie Van Leeuwenhoek 113:197–209

Esquivel DMS, Lins de Barros HGP (1986) Motion of magnetotactic microorganisms. J Exp Biol 121:153–163

Kalmijn AJ (1981) Biophysics of geomagnetic field detection. IEEE Transactions on Magnetics MAG-17 1113–1124

Keim CN, Martins JL, Lins de Barros H, Lins U, Farina M (2006) Structure, behavior, ecology and diversity of multicellular magnetotactic prokaryotes. In: Schuler D (ed) Magnetoreception and Magnetosomes in bacteria. Springer-Verlag, Berlin Heidelberg, pp 103–132. https://doi.org/10.1007/7171_040

Keim CN, De Melo RD, Almeida FP, Lins de Barros HGP, Farina M, Acosta-Avalos D (2018) Effect of applied magnetic fields on motility and magnetotaxis in the uncultured magnetotactic multicellular prokaryote 'Candidatus Magnetoglobus multicellularis'. Environ Microbiol Rep 10(4):465–474

Lins U, Freitas F, Keim CN, Lins de Barros H, Esquivel DMS, Farina M (2003) Simple homemade apparatus for harvesting uncultured magnetotactic microorganisms. Braz J Microbiol 34:111–116

Perantoni M, Esquivel DMS, Wajnberg E, Acosta-Avalos D, Cernicchiaro G, Lins de Barros H (2009) Magnetic properties of the microorganism Candidatus Magnetoglobus multicellularis. Naturwissenschaften 96:685–690

Pichel MP, Hageman TAG, Khalil ISM, Manz A, Abelmann L (2018) Magnetic response of Magnetospirillum gryphiswaldense

observed insede a microfluidic channel. J Magn Magn Mater 460:340–353

Rosenblatt C, Torres de Araujo F, Frankel RB (1982) Birefringence determination of magnetic moments of magnetotactic bacteria. Biophys J 40:83–85

Wang Y, Casaburi G, Lin W, Li Y, Wang F, Pan Y (2019) Genomic evidence of the illumination response mechanism and evolutionary history of magnetotactic bacteria within the Rhodospirillaceae family. BMC Genomics 20:407

Zhu XJ, Ge X, Li N, Wu LF, Luo CX, Ouyang Q, Tu Y, Chen G (2014) Angle sensing in magnetotaxis of *Magnetospirillum magneticum* AMB-1. Integr Biol 6:706–713